Phase–Lifetime Spectrophotometry of Deoxycholate-Purified Bacteriorhodopsin Reconstituted into Asolectin Vesicles†

John Krupinski and Gordon G. Hammes*

Section of Biochemistry, Molecular and Cell Biology and Department of Chemistry, Cornell University, Ithaca, New York 14853

Received May 3, 1985

ABSTRACT: A rapid reconstitution procedure has been developed to insert deoxycholate-purified bacteriorhodopsin (bR) into asolectin vesicles. The procedure relies on the ability of the hydrophobic resin Bio-Beads SM-2 to remove octyl glucoside from a mixture of deoxycholate-purified bR, asolectin, and the detergent. Light-dependent acidification of the vesicle interior is observed with the reconstituted preparations as judged by the fluorescence quenching of an entrapped pH indicator, pyranine. Inhibition of proton pumping by the addition of $LaCl_3$ to the external medium indicates that approximately 90% of the bR is oriented such that it pumps protons into the vesicles. Phase–lifetime spectrophotometry was used to study the relaxation processes associated with the intermediate in the photocycle of the reconstituted bR which absorbs at 410 nm. Amplitude spectra indicate that these absorbance changes are associated with the M intermediate in the bR photocycle. Two relaxation processes are observed. One is characterized by a relaxation time of approximately 4 ms and is independent of pH over the range 4.4–9.4. The longer relaxation time varies from 4 to 200 ms in the same pH range. By digitization of transients, which are observable when the actinic source is modulated at a low frequency, information about the dependence of the slower process on the light intensity and carbonyl cyanide *m*-chlorophenylhydrazone was obtained. The results can be interpreted in terms of two different forms of the M intermediate that decay on parallel kinetic paths. To explain the pH dependence of the decay rate, the slower decaying form must have three coupled protonation states, each with a different decay rate.

The light-driven proton pump bacteriorhodopsin (bR)[1] is the only protein present in the purple membrane isolated from *Halobacterium halobium* [for review, see Stoeckenius & Bogomolni (1982)]. It is a retinylidene protein that undergoes a complex photoreaction cycle. In addition to the ground state, bR_{570}, at least four intermediates, K_{630}, L_{550}, M_{410}, and O_{640}, are observed transiently upon illumination. The widely separated absorbance maxima of the intermediates (wavelengths in nanometers are indicated by the subscripts) have made bR an attractive system for photochemical investigations. In particular the M intermediate, which dominates in the millisecond region, has been studied intensively. The release of a proton from the Schiff-base linkage of the chromophore has been correlated with the formation of M (Lewis et al., 1974). However, additional protons must be involved to account for ratios of protons pumped per M formed which exceed unity (Govindjee et al., 1980; Stoeckenius et al., 1981).

The reconstitution of bR into phospholipid vesicles results in a simple system that offers the opportunity to study both the photocycle and the electrochemical proton gradient generated upon illumination. Many methods exist for reconstituting bR (van Dijck & van Dam, 1982). In this work a rapid method of reconstitution is presented. The preparation that results generates a large proton gradient, as judged by the light-dependent fluorescence quenching of an entrapped pH indicator, pyranine. The kinetics of the M intermediate in the reconstituted system are then studied by a new technique, phase–lifetime spectrophotometry.

Phase–lifetime spectrophotometry has been proposed as a method for studying light-dependent, ion pumping systems (Dewey & Hammes, 1981). The technique involves the measurement of variations in the amplitude of a continuous measuring beam that occur in response to a periodically modulated actinic source. When the modulation occurs on a time scale comparable to the lifetime of the process being monitored, the amplitude will decrease as a function of increasing modulation frequency (Eigen & De Maeyer, 1974). Alternatively lifetimes can be calculated by measuring the phase angle that characterizes the lag between the actinic light and the system response. Phase–lifetime spectrophotometry is related to modulation excitation spectrophotometry (Slifkin & Walmsley, 1970), but the use of amplitude data in phase–lifetime makes the resolution of multiple lifetimes a simpler task. Since the illumination establishes a photostationary state, the experimental conditions are more nearly physiological than those of flash photolysis.

In the present study, a phase–lifetime spectrophotometric investigation is performed with deoxycholate-purified, reconstituted bR. Two processes are observed. One has a lifetime of 4 ms and is largely insensitive to pH. The other varies from about 4 to 200 ms in the pH range 4.4–9. The phase–lifetime technique is also extended by the direct digitization of the transients that arise from illumination at low chopping frequencies. This allows additional information about the slow process to be obtained. These results are discussed in terms of specific mechanistic implications for the reconstituted

† This work was supported by a grant from the National Institutes of Health (GM 13292).

* Address correspondence to this author at the Department of Chemistry.

[1] Abbreviations: bR, bacteriorhodopsin; pyranine, 8-hydroxy-1,3,6-pyrenetrisulfonate; CCCP, carbonyl cyanide *m*-chlorophenylhydrazone; Tris, tris(hydroxymethyl)aminomethane.

0006-2960/85/0424-6963$01.50/0

preparation of bR as well as general considerations for the application of phase–lifetime spectrophotometry.

Materials and Methods

Chemicals. Concentrated soybean phospholipids (asolectin) were from Associated Concentrates. Bio-Beads SM-2 were obtained from Bio-Rad Laboratories. Sephadex G-50 fine was from Pharmacia Fine Chemicals. 1,3,6,8-Pyrenetetrasulfonate and 8-hydroxy-1,3,6-pyrenetrisulfonate were from Molecular Probes. Octyl β-D-glucopyranoside was from Calbiochem-Behring. The following were obtained from Sigma Chemical Co.: sodium deoxycholate, valinomycin, CCCP, *N*-(2-hydroxyethyl)piperazine-*N*′-2-ethanesulfonic acid, 2-(*N*-morpholino)ethanesulfonic acid, Tris, L-arginine (free base), L-glutamic acid (free acid), sodium azide, and Triton X-100. All other chemicals were high-quality commercial grades.

Bacteriorhodopsin. Halobacterium halobium strain S9-P, a gift from Dr. Aaron Lewis, Cornell University, was grown on a peptone medium (Lanyi & MacDonald, 1979). Purple membrane was isolated according to Oesterhelt & Stoeckenius (1974), except that the sucrose step gradient of Becher & Cassim (1975) was used in the final step. The concentration of bR was determined spectrophotometrically by use of an extinction coefficient of 54 000 M^{-1} cm^{-1} at 560 nm and a molecular weight of 26 000 (Oesterhelt & Stoeckenius, 1974). One-milligram aliquots of purple membrane were frozen in sucrose at −20 °C. Thawed aliquots were freed of sucrose by diluting them to approximately 25 mL with the desired buffer, pelleting the purple membrane by centrifugation at 176000*g* for 30 min at 4 °C in a Beckman 60 Ti rotor, and resuspending the pellet in buffer to a final concentration of 2 mg/mL. For most of the work the bR was further purified with deoxycholate (Hwang & Stoeckenius, 1977). This procedure removes about 80% of the endogenous lipid in the purple membrane and replaces it with deoxycholate.

Reconstitution of bR into Phospholipid Vesicles. bR was incorporated into phospholipid vesicles by using Bio-Beads SM-2 to remove octyl glucoside from a bR–lipid–detergent mixture. Asolectin liposomes were prepared at a concentration of 10 mg/mL in either buffer A or buffer B. Buffer A consisted of 0.01 M 2-(*N*-morpholino)ethanesulfonic acid, 0.01 M *N*-(2-hydroxyethyl)piperazine-*N*′-2-ethanesulfonic acid, 0.02 M L-arginine, 0.03 M sodium azide, and 0.12 M KCl, pH 8.0. Buffer B was 0.01 M L-glutamic acid, 0.01 M 2-(*N*-morpholino)ethanesulfonic acid, 0.02 M Tris, 0.03 M sodium azide, and 0.12 M KCl, pH 8.0. The asolectin suspension was vortexed under nitrogen for 5 min and then sonicated in a bath type sonicator (Laboratory Supplies Co.) until only a slight opalescence remained. The addition of 73 μL of 0.5 M octyl glucoside to 0.5 mL of liposomes resulted in a clear solution. This mixture was chilled on ice. At time zero the detergent–lipid solution was added to 0.5 mL of cold solution containing 1 mg of deoxycholate-purified bR in the appropriate buffer. Final concentrations were the following: deoxycholate-purified bR, 1 mg/mL; asolectin, 5 mg/mL; octyl glucoside, 10 mg/mL. After a 10-min incubation on ice, the solution was applied to a 1.5 × 8 cm column containing 6 g of Bio-Beads SM-2. The beads were preequilibrated as described previously (Holloway, 1973), with a final wash of 5 column volumes of buffer. The bR–lipid mixture was eluted from the column with buffer at a rate of 0.3 mL/min. The turbid purple fraction was collected and applied to a 1.5 × 8 cm column of Sephadex G-50 fine equilibrated with the appropriate buffer. Again the fraction containing chromophore was collected upon elution with buffer. For individual experiments, the pH of the solution was adjusted by addition of either 1 M KOH or 1 M HCl and stirred for 1 h before the start of an experiment. Buffer A was used for pH 6–9 and buffer B for pH 4–6.

For some experiments the fluorescent pH indicator 8-hydroxy-1,3,6-pyrenetrisulfononate (pyranine) was trapped inside the vesicles. This was done by forming asolectin vesicles as described above except that 0.01 M pyranine and 0.12 M KCl, pH 8.0, was used instead of the usual buffers and the Bio-Beads column was equilibrated with 0.12 M KCl. Subsequent passage through the Sephadex G-50 column (as described above) separated free indicator from trapped indicator and also made the conditions of the external solution identical with those used in the standard reconstitution. The vesicles were diluted such that the final concentrations were 0.07 mg/mL bR, 0.33 mg/mL asolectin, and approximately 2 μM pyranine in 2.5 mL of buffer. The concentration of pyranine was estimated by comparing the fluorescence of entrapped pyranine with that of a stock solution (Kano & Fendler, 1978). This assumes that the entrapped pyranine has a quantum yield and p*K* similar to that of free pyranine in aqueous solution. Where indicated NH_4Cl or $LaCl_3$ was added to the desired concentration from 0.25 M stock solutions in buffer A. CCCP, nigericin, or valinomycin was added from ethanol solutions of 10, 0.25, or 0.1 mM, respectively.

The distribution of bR in the lipid vesicles was characterized by centrifugation on a sucrose gradient. A linear gradient containing 14 mL of 5–35% (w/w) sucrose in buffer A was layered on top of a 1-mL 45% sucrose cushion. The vesicle sample was applied and centrifuged at 116000*g* for 10 h at 4 °C in a Beckman SW 27.1 rotor. Fractions were mixed with an equal volume of 1% Triton X-100. Vesicles were located by monitoring the 510-nm fluorescence of the entrapped pyranine, while the bR was detected by measuring the absorbance at 550 nm.

Another method of reconstitution based on that of Bell et al. (1983) was used for comparison. Sonicated asolectin liposomes containing pyranine were formed as described above. bR was then incorporated into the vesicles by sonicating a mixture of liposomes (final concentration 5 mg/mL) and purple membrane (1 mg/mL) in the pyranine solution. Sonication was continued for 30 min (Bell et al., 1983). External pyranine was removed by passage through a Sephadex G-50 column as described above.

Steady-State Proton Pumping Measurements. The samples described above were used for measurements of proton pumping under steady-state illumination. The sample was placed in a 1 × 1 cm stoppered quartz fluorescence cuvette in a Perkin-Elmer MPF-44 fluorescence spectrophotometer. The cuvette holder was designed such that bR could be illuminated through the front face of the cuvette, while pyranine fluorescence was excited at 460 nm from the rear face. Emission at 510 nm was monitored at a right angle to the light beams. Corrected steady-state fluorescence polarization measurements were performed as described previously (Cerione & Hammes, 1982).

The actinic light source was a Kodak 600 H slide projector with a 300-W ELH lamp. The projector was rewired to run off a Kepco SM-75 DC power supply. The projector beam was focused on the cuvette through an opening in the front cover of the spectrofluorometer. The actinic light was passed through a Corning CS 3-66 filter (which transmits wavelengths >570 nm) and a Corning 1-75 infrared–ultraviolet filter. The incident light intensity on the sample was approximately 10^6 ergs/(cm^2·s) as determined with a YSI-Kettering Model 65 photometer (Radiometer). Where indicated, calibrated neutral

density filters (Ditric Optics) were used to decrease the light intensity of the actinic source. In some experiments the actinic light was modulated with a Bentham Model 218 optical chopper. The pyranine fluorescence was monitored continuously to measure changes in internal pH.

Phase–Lifetime Spectrophotometry. The instrumentation was similar to that reported previously (Dewey & Hammes, 1981; Krupinski et al., 1983). The actinic source was the same as that used in the steady-state proton pumping experiments described above. A Bentham Model 218 optical chopper was placed between the actinic source and the sample cell. The frequency was monitored with a Hewlett-Packard 5221B electronic counter. A 100-W GE Quartzline tungsten–iodide lamp with a Kepco ATE 5510 power supply was positioned at a right angle to the actinic source. The wavelength of this measuring beam was selected with a suitable Ditric narrow band-pass filter. For experiments in which the amplitude was measured as a function of chopping frequency, the absorption maximum of the M intermediate, 410 nm, was chosen. The measuring beam was focused onto the sample with a condensing lens. After exiting from the sample, the beam passed into a Bausch & Lomb 250-mm ultraviolet–visible monochromator adjusted to the same wavelength as the band-pass filter. The intensity variations were detected with an EMI 9635 QB photomultiplier in a Pacific Instruments 62/3A14 housing with a Pacific Instruments 204-03L high-voltage power supply. An Ithaco 393 lock-in amplifier abstracted that component of the photomultiplier output which varied at the same frequency as the chopper. The total intensity of the photomultiplier output was measured on a Tektronix 5441 storage oscilloscope. The amplitude measured with the lock-in amplifier was scaled with the oscilloscope and then was divided by the total intensity to make it dimensionless.

A typical sample consisted of 3 mL of either buffer A or buffer B containing bR vesicles, at final concentrations of 0.33 mg/mL bR and 1.7 mg/mL asolectin. The sample was light-adapted by preilluminating for 10 min at a chopping frequency of 100 Hz. All experiments were carried out in a cuvette holder which was thermostated at 22 °C.

Relaxation times were computed from the variation of the amplitude as a function of frequency by fitting the data to (Dewey & Hammes, 1981; see Appendix)

$$A_{obsd}(\omega) = \sum_{i=1}^{n} \frac{A_{i0}}{\sqrt{1 + \omega^2 \tau_i^2}} \quad (1)$$

where $A_{obsd}(\omega)$ is the observed amplitude, A_{i0} is the maximum contribution to the observed amplitude made by the process characterized by relaxation time τ_i, ω is the chopping frequency in radians per unit time, and n is the total number of processes. In these experiments the points were acquired nonsequentially, and several values were reproduced to check for possible photobleaching. None was observed.

Alternatively the transient rises and decays that occurred in response to the modulated actinic light could be observed directly. A very low (~2 Hz) chopping frequency was used in these experiments. The output of the photomultiplier passed into the storage oscilloscope which was triggered by the electronic reference of the optical chopper. A 200-ms sweep was digitized with a Biomation 802 transient recorder interfaced to a Digital PDP 11/24 computer. Typically 20 transients were signal averaged.

In these experiments the chopping frequency was so slow that the rise time for the perturbation was not negligible. The data were analyzed in terms of the forced solution to the relaxation equation when the forcing function is a step function with a linear increase (Bernasconi, 1976). For a decaying exponential

$$A_{obsd}(t) = -(A_0/t_1)[\tau \exp[(x - t)/\tau] - \tau \exp(-t/\tau) - x] + C \quad (2)$$

Here, $A_{obsd}(t)$ is the observed amplitude, t is the time, τ is the relaxation time of the process, C is the amplitude at $t = 0$, $A_0 + C$ is the amplitude at $t = \infty$, t_1 is the finite rise time of the chopper, and the parameter x is equal to t for $0 < x \leq t_1$ and is equal to t_1 for $t > t_1$. All data fitting was done on a Digital PDP 11/24 computer by a general nonlinear least-squares analysis. Once again the amplitudes were converted to a dimensionless form with the aid of an oscilloscope.

Results

bR Reconstitution. If deoxycholate-purified bR is incubated with a solution of phospholipid and octyl β-D-glucopyranoside, subsequent removal of the detergent results in the formation of bR-containing liposomes. Both monomers and micelles of octyl glucoside can be removed from solution by passage through a column of the hydrophobic resin Bio-Beads SM-2 (Lin et al., 1979). This method results in vesicles that can generate high steady-state proton gradients upon illumination.

The fluorescent pH indicator pyranine can be used to assay the proton pumping activity of the vesicles. The amount of pyranine fluorescence excited at 460 nm and emitted at 510 nm decreases with pH. Vesicles containing bR and entrapped pyranine do not leak dye on the time scale of the experiments reported here. If the vesicles are passed through a Sephadex G-50 column following an experiment, no free pyranine can be separated from the vesicles. However, if the vesicles are stored at 4 °C for 2 days, a second passage through the column separates approximately 12% of the pyranine from the liposomes. Pyranine does not bind significantly to either bR or the lipids. The fluorescence polarization of the entrapped pyranine is 0.017 before illumination and 0.018 during illumination. The difference between these polarization values is within the experimental error in the measurement. These values of the polarization are different than the polarization of pyranine in cationic vesicles where pyranine is known to be bound to the lipid (Kano & Fendler, 1978).

A sucrose density gradient profile of the vesicle preparation is presented in Figure 1. The vesicles run as one continuous zone on the gradient with the peak at approximately 16% sucrose. The peaks of the pyranine fluorescence and the bR absorbance coincide, and the relative distribution of the indicator and the bR are similar. The lack of any significant absorbance at the interface between the 35% and 45% sucrose (fractions 14 and 15) indicates that no free bR is present. If buffer A is used in place of pyranine in the reconstitution procedure, the absorbance profile of the sucrose gradient still shows one peak at 16% sucrose (data not shown). This indicates that the dye does not interfere with the reconstitution.

Figure 2 illustrates the effect of illuminating the vesicles with 570-nm light in the presence of 200 nM valinomycin at pH 7.4. The pyranine fluorescence excited at 460 nm is quenched. The half-time for quenching is 27 s, and the final extent of quenching is 82%. Since the excitation peak at 460 nm is due to the deprotonated form, this corresponds to a net acidification of the vesicle interior. The fluorescence of the protonated form of pyranine, which has an excitation maximum near 400 nm (Kano & Fendler, 1978), increases at the same rate as the decrease at 460 nm (data not shown). In the absence of valinomycin the quenching rate is much slower. After a 10-min illumination the quenching was 71%. The quenching is completely reversible in the dark (Figure 2). The

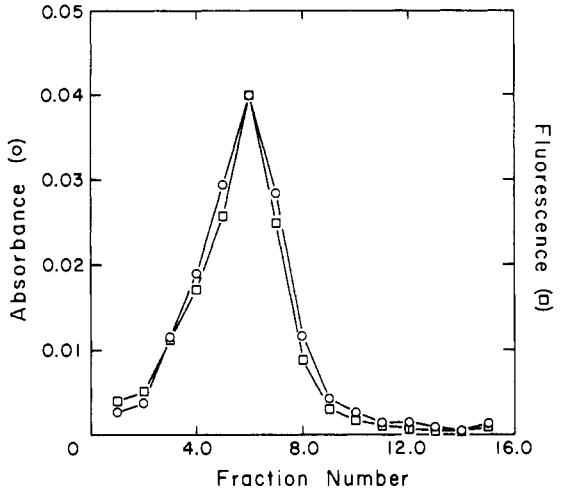

FIGURE 1: Sucrose gradient profile of bR vesicles reconstituted by the Bio-Beads technique. The vesicles contain 0.067 mg/mL bR, 0.33 mg/mL asolectin, and approximately 2 μM pyranine in 1.5 mL of buffer A, pH 8.0. The linear sucrose gradient extends from 5% (w/w in buffer A, fraction 2) through 35% (fraction 14). A 1-mL cushion of 45% sucrose is in fraction 15. The vesicles were centrifuged as described under Materials and Methods. The various fractions were dissolved with an equal volume of 1% Triton X-100 and analyzed for bR absorbance (○) at 550 nm. The vesicles were located by monitoring the 510-nm fluorescence of entrapped pyranine that was excited at 460 nm (□). The arbitrary fluorescence units have been normalized to the same scale as the absorbance units.

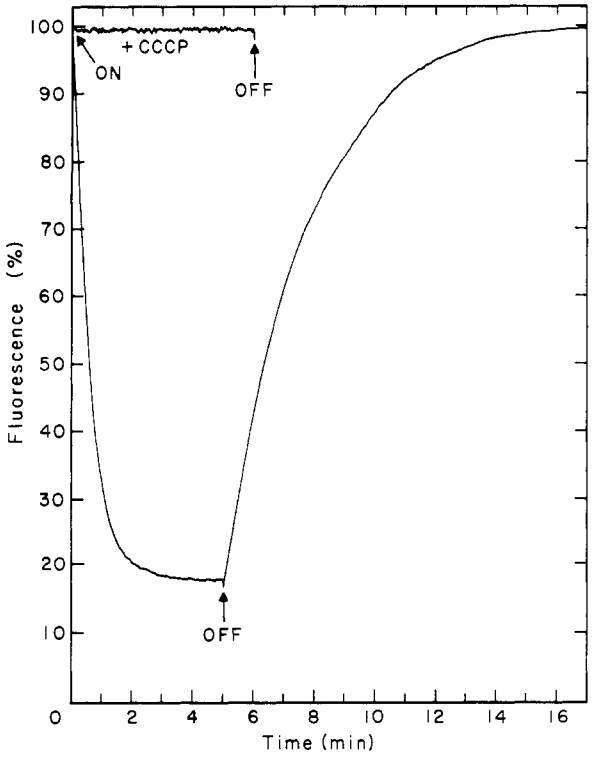

FIGURE 2: Light-induced fluorescence quenching of pyranine entrapped in bR-containing vesicles. The sample consists of 2.5 mL of vesicles with final concentrations of 0.067 mg/mL bR, 0.33 mg/mL asolectin, approximately 2 μM pyranine, and 200 nM valinomycin. The arrows indicate the points at which the actinic source (wavelength >570 nm) was switched on or off. The light intensity was approximately 10^6 ergs/(cm^2·s). The pyranine fluorescence was excited at 460 nm and monitored at 510 nm. The approximately horizontal trace indicates the response of the system when the protonophore CCCP is included at a final concentration of 2 μM.

half-time for recovery is about 2 min in the presence of 200 nM valinomycin. The addition of more valinomycin continues to speed up the rate of recovery, but it decreases the rate of fluorescence quenching.

Table I: Characterization of bR Vesicles[a]

sample	% quenching[b]	$t_{1/2}$ (s)[c]
at pH 7.4		
control	82	27
2 μM CCCP	0	
500 nM nigericin	0	
1 mM $LaCl_3$	43	78
5 mM $LaCl_3$	−10	6
10 mM $LaCl_3$	−10	6
17 mM NH_4Cl	8	12
buffer B	78	25
at pH 8.0		
control	89	63
$^1/_2$ light intensity	83	114
10-Hz light chopping	83	120

[a] bR-containing vesicles (2.5 mL) with entrapped pyranine: 0.067 mg/mL bR, 0.33 mg/mL asolectin, ~2 μM pyranine, and 200 nM valinomycin. Buffer A was used unless otherwise indicated. [b] Final value with a light intensity of ~10^6 ergs/(cm^2·s). [c] Time required to reach half of the final quenching.

If the vesicle population were homogeneous, then the percent quenching could be related quantitatively to ΔpH. However, the presence of bR in different orientations with respect to the vesicle interior (see below) complicates such an analysis. For this reason we report only the final percent quenching and the half-time for the process without attempting to quantify the true internal pH.

Table I includes the results of additional experiments with the pyranine-containing bR vesicles. If either 500 nM nigericin or 2 μM CCCP is added to the vesicles in the presence of 200 nM valinomycin, light-dependent fluorescence quenching is completely abolished (Table I and Figure 2). The addition of 17 mM NH_4Cl decreases the quenching to 8% at pH 7.4 (Table I). Another amine, Tris (present at 20 mM in buffer B), has no significant effect (Table I). This result indicates that the vesicles are more permeable to NH_3 than to Tris. If pyrenetetrasulfonate, a structurally similar fluorescent probe lacking the ionizing hydroxyl that causes the pH dependence of the pyranine fluorescence, is used in the reconstitution instead of pyranine, light-dependent quenching is not observed.

For comparison, vesicles with entrapped pyranine and the same lipid to protein ratio were formed by the sonication technique (see Materials and Methods). The free pyranine was removed by passage through a Sephadex G-50 column as in the procedure that uses Bio-Beads. Even in the presence of 200 nM valinomycin, the sonication vesicles gave only 6.3% fluorescence quenching upon illumination. Therefore, the vesicles formed on the Bio-Beads show more than an order of magnitude increase in the apparent extent of light-induced proton pumping relative to the vesicles obtained by sonication.

At 1 mM, $LaCl_3$ decreases quenching to 43% (Table I). When the concentration is greater than 3 mM, an increase in fluorescence is observed upon illumination. This corresponds to a net alkalinization of the vesicle interior. This effect saturated at about 5 mM (Table I). La^{3+} ions have been shown to inhibit both the M decay and the millisecond phase of the photoelectric response (Drachev et al., 1981). More recently La^{3+} has been shown to replace divalent cations which are specifically bound to bR as it is normally isolated (Chang et al., 1985). This replacement is accompanied by the inhibition of proton uptake. Our results with La^{3+} are consistent with the interpretation that the divalent cations necessary for proton pumping can only be displaced by La^{3+} from the outside of the vesicle. The net alkalinization of the vesicle interior then results from that fraction of the bR which has its orientation reversed relative to the majority and cannot be in-

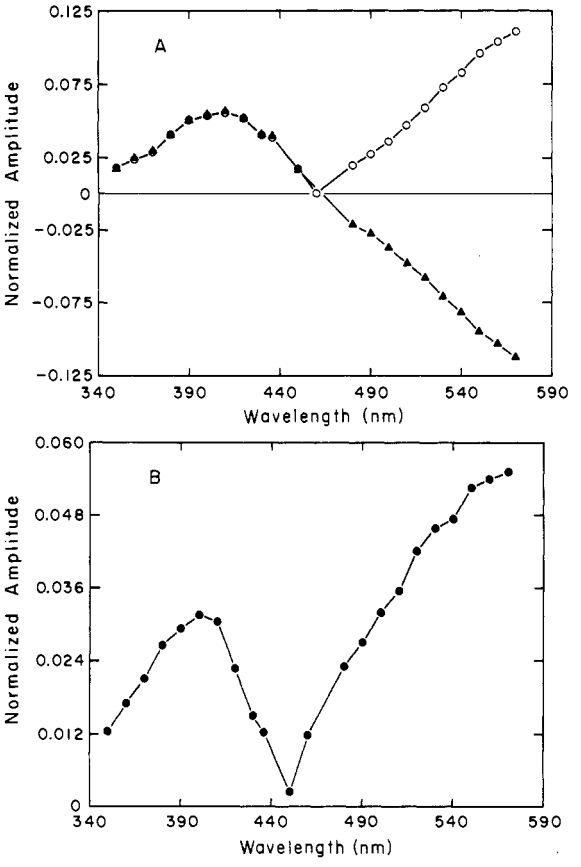

FIGURE 3: Amplitude spectra of deoxycholate-purified bR and reconstituted bR. (A) The sample consists of 0.18 mg/mL bR suspended in 3 mL of buffer A, pH 6.4. The open circles are the normalized amplitudes obtained by phase–lifetime spectrophotometry, whereas the closed triangles are the values determined by digitizing the light-induced transient observed on the oscilloscope. In both cases the constant light chopping frequency was 2 Hz. The amplitudes have been converted to oscilloscope units and divided by the total intensity of the measuring beam to make them dimensionless. The transient amplitudes have been plotted with a change of sign to facilitate comparison since the peak at 410 nm is the region of interest for most of this work. (B) The sample consists of 3 mL of buffer A, pH 6.4, containing bR vesicles at final concentrations of 0.33 mg/mL bR and 1.7 mg/mL asolectin. The amplitudes were determined by the phase–lifetime method with a constant chopping frequency of 4 Hz. For both (A) and (B) the light intensity was approximately 10^6 ergs/(cm^2·s), and the temperature was 22 °C.

hibited by La^{3+}. If the orientation of bR relative to the vesicle interior is assumed to not significantly affect the extent of proton pumping and a linear relationship between pumping and quenching is assumed, then approximately 90% of the bR pumps protons into the vesicles and 10% pumps protons out (Table I, entries 1 and 5).

Since phase–lifetime spectrophotometry relies upon measuring the response of the system to a modulated light source, the effect that chopping the light has on the percent quenching was determined. If the actinic light is chopped at a frequency of 10 Hz, the rate of quenching is decreased by a factor of 2 (Table I). If the intensity of the actinic light is halved with a calibrated neutral density filter, then the rate of fluorescence quenching is also halved. These results are consistent with the interpretation that the acidification of the vesicle interior is proportional to the amount of actinic light being absorbed by bR and that the acidification of the bulk phase is slow relative to the time scale of chopping.

Phase–Lifetime Spectrophotometry. In Figure 3A an amplitude spectrum of deoxycholate-purified bR is presented. Results obtained with both the phase–lifetime and transient methods are shown. The conditions are given in the figure legend. Data could not be acquired at wavelengths greater than 570 nm because scattering from the actinic source resulted in a frequency-independent amplitude. The magnitude of the amplitudes determined with the lock-in amplifier and that determined by directly recording transients are in excellent agreement with one another. The only discrepancy is one of sign. The data obtained by recording the transient amplitudes at 2 Hz have been plotted with a change of sign to facilitate comparison and so that the data more nearly resemble a conventional absorbance action spectrum of bR obtained by flash photolysis (Lozier et al., 1975). The lock-in amplifier only reports the absolute value of the amplitude. However, the phase angle of the signal determined by the lock-in amplifier changes sign relative to the chopper reference when the measuring wavelength is greater than approximately 460 nm. This indicates that, in the light, the species with an absorption maximum at 410 nm, probably the M intermediate, is being generated while the species with maximum absorbance at 570 nm, the bR ground state, is being depleted.

Figure 3B shows the amplitude spectrum for reconstituted, deoxycholate-purified bR as a function of wavelength. At 4 Hz there is a broad, asymmetric peak with a maximum at 400 nm. The amplitude reaches a minimum near 450 nm and then rises continuously to the longest wavelength, 570 nm.

Figure 4A shows the response, at 410 nm, of reconstituted, deoxycholate-purified bR to the modulated actinic source. The exact conditions are given in the figure legend. Upon illumination, the intensity of transmitted 410-nm light decreases, which indicates an increase in the concentration of the intermediate. The decay is not a pure exponential since a very low chopping frequency had to be used to view the entire decay. The rise time for the perturbation is not negligible relative to the time scale of the process. Therefore, the finite rise time has been included explicitly in fitting the data (eq 2). The computed relaxation time, τ, is 58 ± 2.5 ms while the rise time, t_1, is 7.5 ± 0.9 ms. (The standard deviation is computed from several different experiments.) The complete set of parameters calculated by a nonlinear least-squares fit to eq 2 is included in the figure legend. A rise in intensity occurs as the chopper blocks the actinic beam and the intermediate decays (Figure 4A). One relaxation time has been used to fit this trace also. Its value is 88 ± 3 ms, while the rise time agains is found to have a value of 7.5 ± 0.8 ms. The systematic errors in the initial region of the curve may be a result of the fact that the rise of the chopper is not adequately represented as a linear increase followed by a constant. If the transient data are fit to two lifetimes, the fit of the data is not significantly improved. Note that the amplitude of the rise matches that of the decay, indicating that the system is in a photostationary state.

Figure 4B shows a plot of the amplitude of the modulated intensity change of the bR vesicles measured with the lock-in amplifier as a function of the chopping frequency. Since the chopping frequencies used (approximately 2–500 Hz) span a range comparable to and faster than the time scale of the bR response shown in Figure 4A, the amplitude decreases as a function of frequency. If the data are fit to eq 1, two relaxation processes are required to fit the data satisfactorily. If only one time constant is used, the calculated curve lies below all of the experimental points at frequencies greater than approximately 25 Hz. This systematic error indicates the presence of a faster process. The slower relaxation time, 72 ± 3.7 ms, is between the two relaxation times calculated for the rise and decay shown in Figures 4A. The Ithaco 393

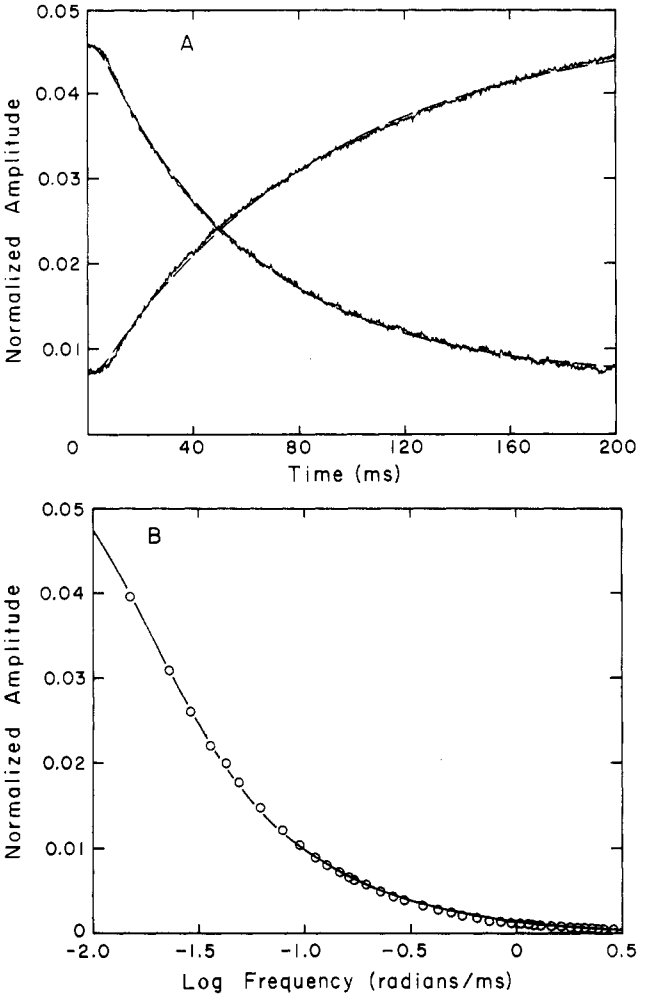

FIGURE 4: Amplitude at 410 nm of reconstituted bR as a function of time or chopping frequency. (A) System response at 2 Hz as a function of time. The sample consists of 3 mL of buffer A, pH 7.5, with bR at 0.33 mg/mL and asolectin at 1.7 mg/mL. The dashed lines are the best fit to eq 2. For the decaying component, which appears upon illumination of the system with 570 nm light, A_0 = −0.0394, τ = 58.3 ms, t_1 = 7.5 ms, and C = 0.0459. The rise in intensity occurs when the actinic light is blocked by the chopper. The parameters for the rise are A_0 = 0.0412, τ = 87.9 ms, t_1 = 7.5 ms, and C = 0.0071. (B) The system response at 410 nm was examined as a function of the chopping frequency. The sample was the same as that in (A). The curve was obtained by a nonlinear least-squares fit to eq 1 with i = 2. A_{10} = 0.0023, τ_1 = 4.1 ms, A_{20} = 0.0556, and τ_2 = 72.4 ms. For both (A) and (B), the light intensity was approximately 10^6 ergs/(cm^2·s), and the sample was thermostated at 22 °C.

lock-in amplifier used in these studies reports the root mean square average amplitude of the first Fourier component of the signal over one entire cycle. Since the cycle includes both a rise and a decay, the amplitude should depend on the lifetimes of both processes. In fact the average of the rise and decay relaxation times from the transient measurements is 73.1 ms, in good agreement with the time constant of the slower process observed with the phase method. The two relaxation times observed with the phase–lifetime method cannot be resolved from the transient data in Figure 4A. The lifetime of the faster relaxation process, 4.1 ± 0.9 ms, computed from the data in Figure 4B only makes a 4% contribution to the total amplitude but is essential to fit the high frequency data. Its small relative weight and the fact that it occurs during the rise time of the light chopping at low frequencies explain why this process cannot be resolved when the transient response of the system is observed directly.

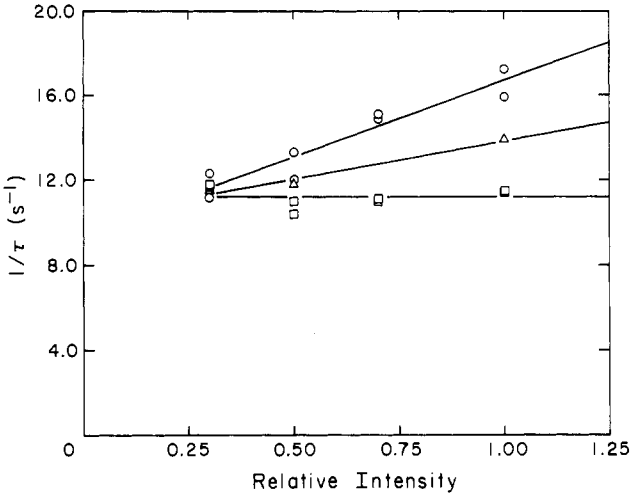

FIGURE 5: Plot of $1/\tau$ or $1/\tau_2$ as a function of the relative light intensity. The sample is that of Figure 4. The light intensity corresponding to 1.0 on the relative scale is approximately 10^6 ergs/(cm^2·s). The other intensities were obtained by using calibrated neutral density filters. The circles are the relaxation times (τ) obtained by fitting the transients at 2 Hz when the actinic light is illuminating the vesicles. The squares are the relaxation times (τ) obtained from the transient measurements when the chopper is blocking the actinic light. The triangles are the relaxation times (τ_2) calculated for the slow process from phase–lifetime measurements after a full frequency dependence was obtained as in Figure 4B.

Figure 5 shows a plot of $1/\tau$ (transient measurements) or $1/\tau_2$ (phase measurements) as a function of the relative light intensity. The reciprocal relaxation time for the decay of the intermediate with the light off is independent of intensity with an average value of 11.2 ± 0.4 s^{-1}. The relaxation time for the rise of the concentration of intermediate with the light on is equal to that for the decay at a relative light intensity of 0.3. At greater intensities, the reciprocal relaxation time increases with intensity. The relaxation time for the slow process determined by phase–lifetime measurements shows the averaging effect discussed above. The short relaxation time determined by phase–lifetime did not show any appreciable intensity dependence. The average lifetime was 3.9 ± 0.5 ms over the entire intensity range.

The effects of varying the light intensity under steady-state illumination are complicated by the development of a protonmotive force. Experiments performed at pH 7.2 in the presence and absence of 10 μM CCCP illustrate this point. At full intensity [$\sim 10^6$ ergs/(cm^2·s)] in the absence of CCCP, the two time constants observed with the phase–lifetime method are 53 ± 4 ms and 3.5 ± 0.6 ms with relative amplitudes of 0.95 and 0.05, respectively. The transient method at a 2-Hz chopping frequency gives relaxation times of 44 ± 3 ms for the light-on phase and 73 ± 6 ms for the light-off phase. The addition of 10 μM CCCP has a significant effect on the observed kinetics. The two time constants determined by phase–lifetime are 35 ± 3 ms and 3.6 ± 0.8 ms with relative amplitudes of 0.92 and 0.08. The relaxation time of the transient light on process is 35 ± 6 ms. The time constant for the light-off process is decreased to 37 ± 5 ms.

The pH dependence of the kinetic process also was determined. Experiments similar to that shown in Figure 4, but at different pH values, were carried out over the pH range 4.4–9.4. The fast process and its absolute amplitude are largely independent of pH over the range 5.0–9.4, even at full light intensity. The average relaxation time is 3.6 ± 1 ms, whereas the average value for the modulated amplitude divided by the total transmitted intensity (A_{10}, eq 1) is 0.002 ± 0.0006 (28 experiments; data not shown).

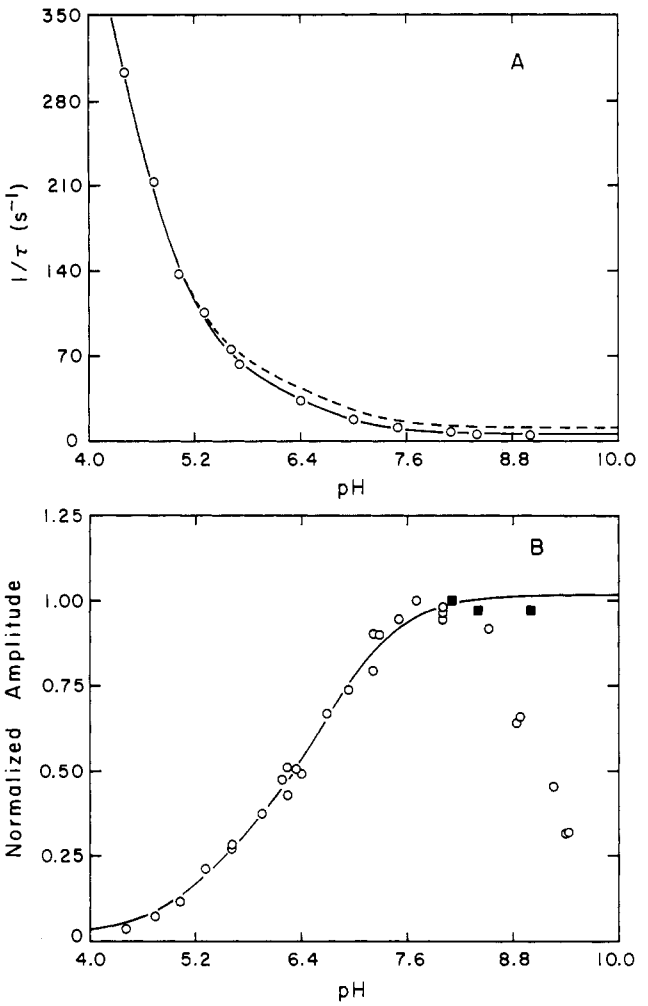

FIGURE 6: pH dependence of the kinetic parameters associated with bR vesicles obtained with the phase–lifetime method. The sample contained vesicles at final concentrations of 0.33 mg/mL bR and 1.7 mg/mL asolectin in 3 mL of buffer A (pH 6–9) or buffer B (pH 4–6). The temperature was 22 °C. (A) Plot of $1/\tau$ as a function of pH. The intensity-independent relaxation time was determined at each pH by performing experiments as in Figure 5 and determining the value at which the relaxation times for the "on" process, the "off" process, and the slow process (τ_2) observed in phase–lifetime were equal. The curve was calculated with eq 4, and the best-fit parameters are given in the text. The dashed line corresponds to the pH dependence observed at full light intensity. The best-fit parameters are given in the text. (B) Amplitude of the slow process (A_{20}) determined by phase–lifetime measurements as a function of pH. The open circles are the values obtained at full light intensity, whereas the closed squares were obtained at a relative intensity of 0.15. The amplitudes have been divided by the maximum observed amplitude so that they could be compared more readily. For the amplitude at full intensity the maximum value was 0.0588 in the dimensionless units of Figure 3. At a relative intensity of 0.15 the maximum value was 0.0040. The curve was calculated with eq 5, and the best-fit parameters are given in the text. Data obtained at pH values greater than 8.0 were excluded from the fitting procedure as discussed in the text.

As shown in Figure 6A, the long relaxation time is pH dependent. Since the associated relaxation process is intensity dependent, several experiments were performed at different intensities, and the pH dependence of the light-independent relaxation time was determined. In all cases the light-off relaxation time is independent of intensity. The relaxation time of the light-on process converges to that of the light-off process at low intensity as in Figure 5. Experiments at pH less than 4.4 could not be carried out since the total amplitude becomes very small (Figure 6). Furthermore, since the relaxation time for the "slower" process becomes comparable to that for the "faster" process at low pH, only one relaxation time was used to fit the data in experiments at pH values less than 5. The data in Figure 6A represent the light-independent relaxation times obtained from both the transient and phase–lifetime measurements (cf. Figure 5). The dashed curve in Figure 6A represents the data obtained with the phase–lifetime method at full light intensity.

The amplitude of the slow process determined with the phase–lifetime method at full light intensity is shown in Figure 6B. At a relative intensity of 0.15 the amplitude of the slow process was independent of pH in the range pH 8.1–9.0 (Figure 6B, closed squares). This indicates the decrease in amplitude at high pH values may be an artifact due to the high light intensity. This matter is discussed further.

Discussion

The Bio-Beads SM-2 reconstitution procedure described in this work is a straightforward method for forming bR-containing phospholipid vesicles. The preparation that results runs as a single zone on a sucrose density gradient (Figure 1), indicating some degree of homogeneity. However, the question of functional homogeneity must be addressed also.

In their study of bR reconstituted by the sonication method, Bell et al. (1983) calculated that even under optimal conditions only 68% of the vesicles appeared to be capable of generating a light-dependent pH gradient. An increase in the relative percentage of active vesicles in our preparation would readily explain the efficiency of the Bio-Beads reconstitution relative to the sonication method. The reason for this increase is unknown, but deoxycholate-purified bR generates larger pH gradients upon illumination than reconstituted purple membrane fragments (Hwang & Stoekenius, 1977; Huang et al., 1980; van Dijck & van Dam, 1982). The experiments with $LaCl_3$ (Table I) indicate that the Bio-Beads preparation has approximately 90% of the bR oriented such that it pumps protons into the vesicle. This is comparable to the best reconstitutions previously reported (Hwang & Stoeckenius, 1977; Huang et al., 1980).

The vesicles must be leaky to some small ions since they are capable of quenching greater than 70% of the initial pyranine fluorescence after a 10-min illumination in the absence of valinomycin. Kinetic studies performed on pure lipid vesicles formed by using a similar hydrophobic resin, XAD-2, from mixtures of octyl glucoside and egg lecithin showed that the vesicles exhibit a substantial chloride permeability (Ueno et al., 1984). Nevertheless, this ion permeability may be increased further since the addition of 200 nM valinomycin increases the rate of light-dependent quenching and light-independent recovery. The concentration of valinomycin used in the experiments presented in Table I, 200 nM, is insufficient to fully relieve the light-induced membrane potential. This is indicated by the fact that the leak rate with the light off continues to increase with increasing valinomycin concentration, although the quenching rate upon illumination actually decreases. This latter fact can be interpreted in terms of a direct inhibition of the M decay by valinomycin (Sherman et al., 1976; unpublished results). The other ionophores examined, CCCP, nigericin, and NH_4Cl, all result in the inhibition of light-dependent quenching in the presence of valinomycin as expected (Table I).

The residual membrane potential in the quenching experiments also explains the results obtained at half the full light intensity and with a chopped actinic source (Table I). They are consistent with the interpretation that the rate of acidification of the vesicle interior is proportional to the amount of actinic light being absorbed by bR and that the rate of acidification of the bulk phase is slow relative to the time scale

of light chopping. This result indicates that, at a given external pH, phase–lifetime spectrophotometric measurements can be performed over a wide frequency range with a constant steady-state ΔpH.

Flash photolysis investigations have shown that deoxycholate-purified bR exhibits the same photocycle intermediates as purple membrane, but with altered kinetics (Lozier et al., 1976; Hwang & Stoeckenius, 1977). Our results are consistent with these previous studies. In Figure 3A the amplitude spectrum of deoxycholate-purified bR shows a peak at 410 nm characteristic of the M intermediate observed in purple membrane fragments (Lozier et al., 1975). The ratio of the amplitude at 570 nm to that at 410 nm is 1.9 (Figure 3A). This is identical with the value found for purple membrane fragments suspended in basal ether salts (Oesterhelt & Hess, 1973) or in aqueous solution (Goldschmidt et al., 1976). Also the location of the isosbestic point near 460 nm is consistent with these studies. Comparison of panel A with panel B of Figure 3 clearly demonstrates that reconstitution alters the M spectrum. The peak of the M spectrum is blue shifted to 400 nm. The ratio of the amplitude at 570 nm to that at 400 nm is only 1.75, while phase information reveals that the isosbestic point is shifted to 452 nm.

Since this is the first report of kinetic investigations on this particular reconstituted preparation of bR, a direct comparison with other work is not possible. However, the observation of multiphasic kinetics with processes occurring in the millisecond time regime has been reported in flash photolysis studies of both purple membrane fragments and other reconstituted preparations of bR (Lozier et al., 1976; Govindjee et al., 1980). Under the conditions given in the legend to Figure 4, unreconstituted, deoxycholate-purified bR also exhibits biphasic kinetics in phase–lifetime experiments. Therefore, the biphasic kinetics does not result from the reconstitution procedure.

The addition of 10 μM CCCP only increases the relative contribution of the fast decaying form from 5% to 8%. However, the longer relaxation time is decreased significantly by the protonophore. Although the phase–lifetime measurements suggest that the effect is less than the factor of 2 found in flash photolysis studies (Groma et al., 1984; Westerhoff & Danschâzy, 1984), the transient measurements indicate the source of this discrepancy. The transient process occurring in the light is barely affected by CCCP (see Results), while the relaxation time of the process with the light off is decreased by a factor of 2. Due to the averaging affect which occurs in phase–lifetime measurements, a relatively small change in the relaxation time is seen.

A simple theoretical analysis of phase–lifetime spectrophotometry predicts that the time constants for the light-on and light-off phases should be the same provided the ground state is not depleted significantly by the perturbation (see Appendix). The data in Figure 4A are inconsistent with this prediction. If the intensity changes are converted to absorbances and a differential extinction coefficient for M of 23000 M^{-1} cm^{-1} at 410 nm (Lozier et al., 1976) is assumed, the calculated fraction of bR cycling through M in the photostationary state is about 10% under the conditions given in the figure legend. If the intensity is reduced to 0.3 of its original value, a limit is reached in which the theory is applicable (Figure 5). However, even under conditions in which the perturbation of the ground state is small, the kinetics may be complicated by the electrochemical proton gradient. At a given external pH, the electrochemical effects must be constant at the light intensities used since the reciprocal relaxation time for the transient process with the light off is independent of intensity (Figure 5). The variation of this intensity-independent reciprocal relaxation time with external pH leads to mechanistic considerations for reconstituted bR cycling in a photostationary state.

The data presented in Figure 6 require the existence of three different protonated states of the slower decaying M form, each of which is capable of decaying to a new state. The simplest mechanism consistent with the data is

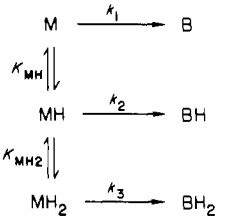

(3)

where the K's are dissociation constants for the protolytic steps, the k_i's are rate constants, and protons have not been explicitly shown for the sake of simplicity. The intermediate following M has not been studied here so it has been designated simply as B. Other work has shown that it is O_{640} in the usual bR nomenclature (Lozier et al., 1975).

If the protolytic reactions are assumed to be in rapid equilibrium and the system is in a stationary state, then the smallest reciprocal relaxation time for the mechanism of eq 3 is (Eigen & De Maeyer, 1974)

$$1/\tau = \frac{k_3 + k_2K_{MH2}/[H^+] + k_1K_{MH}K_{MH2}/[H^+]^2}{1 + K_{MH2}/[H^+] + K_{MH}K_{MH2}/[H^+]^2} \quad (4)$$

If the data in Figure 6A are fit to this equation, the best-fit values of the parameters are $k_1 = 5.6\ s^{-1}$, $k_2 = 51\ s^{-1}$, $k_3 = 580\ s^{-1}$, $pK_{MH} = 6.5$, and $pK_{MH2} = 4.4$. The dashed line in Figure 6A represents the results obtained at full light intensity (28 experiments; data not shown). The only parameter that is altered significantly in this fit is the constant value which the reciprocal relaxation time approaches at high pH, k_1. At full intensity, $k_1 = 11\ s^{-1}$, $k_2 = 57\ s^{-1}$, $k_3 = 606\ s^{-1}$, $pK_{MH} = 6.6$, and $pK_{MH2} = 4.3$. While the identity of these titratable groups remains unknown, recent evidence suggests that the modification of carboxyl groups results in the formation of blue membranes that have photochemical properties identical with those of blue membranes formed at low pH (Chang et al., 1985). In particular blue membranes do not form significant amounts of M upon illumination. If the observed pK values are characteristic of these carboxyl groups, the decreased amplitude of M which occurs at low pH can be understood (Figure 6B).

The pH dependence of the amplitude of the slow relaxation process (Figure 6B, circles) is difficult to interpret quantitatively because reliable data cannot be obtained over the entire pH range at low light intensities. The simplest interpretation of the data is that the drop-off in amplitude at high pH and high light intensity is an artifact due to deviation from the linearized rate equations. In this case, the data can be analyzed in terms of the mechanism in eq 3:

$$A_{20} = \frac{A_{MH2} + A_{MH}K_{MH2}/[H^+] + A_MK_{MH2}K_{MH}/[H^+]^2}{1 + K_{MH2}/[H^+] + K_{MH2}K_{MH}/[H^+]^2} \quad (5)$$

The amplitudes A_{MH2}, A_{MH}, and A_M are proportional to the maximum concentrations of MH_2, MH, and M, which in turn are proportional to the quantum yields for their production. If the data below pH 8.0 in Figure 6B are fit to eq 5, the best-fit parameters are $A_{MH2} = 0.02$, $A_{MH} = 0.36$, $A_M = 1.0$, $pK_{MH2} = 5.4$, and $pK_{MH} = 6.7$. The curve in Figure 6B has

been calculated with these parameters and eq 5. The apparent pK values differ from those obtained by the kinetic analysis of $1/\tau$: for pK_{MH} the difference is only 0.1, which is not significant, but for pK_{MH2} the difference is 1. However, the apparent pK values obtained from the amplitude and relaxation time analyses need not be identical since even for simple mechanisms (Appendix) the amplitude contains a ratio of rate constants and a quantum yield, both of which may be pH dependent. The pK values obtained from the analysis of $1/\tau$ are probably more meaningful, although they suffer from the usual ambiguities arising from kinetic analyses. An alternative analysis of the relaxation amplitude is that the drop off at high pH is due to an ionizable group that is only exposed at high light intensities and does not influence $1/\tau$. This would require deprotonation of an ionizable group with a pK of about 9. This explanation does not seem very likely.

The results reported here require at least four forms of M which are capable of photocycling: the pH-independent fast decaying form and the three different protonation states of the slower cycling M species. All of the data can be most easily accommodated in terms of a mechanism in which the fast and slow decaying forms of M occur on parallel paths resulting from a branch in the photocycle generated from the ground state (Scheme III in the Appendix). Two distinct forms of M have been proposed previously on the basis of several lines of evidence (Slifkin & Caplan, 1975; Hess & Kuschmitz, 1977; Groma et al., 1984; Ohno et al., 1981; Lozier et al., 1976; Govindjee et al., 1980; Li et al., 1984). These observations have led to the proposal that the slow decaying form of M is on the productive proton pumping pathway while the fast decaying form does not pump protons (Groma et al., 1984; Li et al., 1984). The work presented here is consistent with the interpretation that a similar mechanism is operative in the deoxycholate-purified, reconstituted bR system. Thus, phase–lifetime spectrophotometry may be applied to light dependent systems to give results that complement those obtained by other photochemical methods.

ACKNOWLEDGMENTS

We thank Dr. J. L. Rigaud for suggesting the $LaCl_3$ experiments to determine the relative orientation of bR in the vesicles. Numerous individuals have taken part in valuable discussions of the experiments and theory presented in this work. In particular, we thank Drs. B. G. Cox, J. A. H. Cognet, T. G. Dewey, and J. G. Koland.

APPENDIX

Derivation of the Rate Equations. Comparison of the experimental results with the solutions to the rate equations for several simple schemes allows mechanistic conclusions to be drawn on the basis of the data. If a photostationary state is assumed, then a complete perturbation analysis of the system in terms of the normal modes of reaction may be performed by standard procedures (Eigen & De Maeyer, 1974; Bernasconi, 1976). However, the simplified theory presented below reveals all of the salient features of the normal mode analysis with minimal mathematical complications.

The perturbation used in the phase–lifetime experiments is an approximately square wave. However, the lock-in amplifier detects only the fundamental Fourier component of this signal. Therefore, the forcing function may be approximated as a sine wave.

Scheme I

$$A \underset{k_2'}{\overset{k_1}{\rightleftharpoons}} B$$

The simplest two-state model is given in Scheme I where k_1 is a rate constant and k_2' is an effective rate constant which will be assumed to be proportional to the light intensity, I_0, and the quantum yield, Φ_0:

$$k_2' = k_2\Phi_0 I_0 \tag{A1}$$

The rate equation for the time dependence of A is

$$-d[A]/dt = k_1[A] - k_2\Phi_0 I_0[B] \sin \omega t \tag{A2}$$

If the total concentration of A and B is C_0, and the perturbation is assumed to lead to an insignificant depletion of the ground state, then

$$[B] = [C_0] - [A] \simeq [C_0] \tag{A3}$$

The solution to eq A2 is given by

$$[A] = \frac{(k_2/k_1)\Phi_0 I_0[C_0] \sin (\omega t - \phi)}{(1 + \omega^2\tau^2)^{1/2}} + \frac{k_2\omega\Phi_0 I_0[C_0] \exp (-k_1 t)}{k_1^2 + \omega^2} \tag{A4}$$

where $\tau = 1/k_1$ and $\cos \phi = k_1/(k_1^2 + \omega^2)^{1/2}$. For $t \gg \tau$ the second, transient term vanishes, and only the first term contributes to the amplitude. This is a general property of the solution to the relaxation equation for a forced system (Eigen & De Maeyer, 1974; Bernasconi, 1976). Scheme I only results in one relaxation process. Since the phase–lifetime data require two relaxation times, a more complex scheme must be considered.

Scheme II

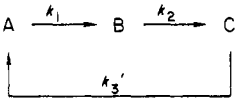

A second possible mechanism is the unidirectional unbranched model given in Scheme II where k_3' is now proportional to the quantum yield and the light intensity. If depletion of the ground state, C, is assumed to be negligible, then

$$-d[A]/dt \simeq k_1[A] - k_3\Phi_0 I_0[C_0] \sin \omega t \tag{A5}$$

The steady-state solution is

$$[A] = \frac{(k_3/k_1)\Phi_0 I_0[C_0] \sin (\omega t - \phi_1)}{(1 + \omega^2\tau_1^2)^{1/2}} \tag{A6}$$

where $\tau_1 = 1/k_1$ and $\cos \phi_1 = k_1/(k_1^2 + \omega^2)^{1/2}$. For intermediate B

$$-d[B]/dt = k_2[B] - k_1[A] = k_2[B] - \frac{k_3\Phi_0 I_0[C_0] \sin (\omega t - \phi_1)}{(1 + \omega^2\tau_1^2)^{1/2}} \tag{A7}$$

The solution is

$$[B] = \frac{(k_3/k_2)\Phi_0 I_0[C_0] \sin \omega t \cos \phi_1 \cos \phi_2}{(1 + \omega^2\tau_1^2)^{1/2}(1 + \omega^2\tau_2^2)^{1/2}} \tag{A8}$$

with $\tau_2 = 1/k_2$ and $\cos \phi_2 = k_2/(k_2^2 + \omega^2)^{1/2}$. If only A is being observed, then one relaxation time, τ_1, will be measured. Two relaxation times are always required to fit the data. Furthermore, in the pH range 6.4–9.4 one relaxation time is at least an order of magnitude greater than the other. If $\tau_1 \ll \tau_2$ and species B is observed

$$[B] = \frac{(k_3/k_2)\Phi_0 I_3[C_0] \sin (\omega t) \cos \phi_1 \cos \phi_2}{(1 + \omega^2\tau_2^2)^{1/2}} \tag{A9}$$

and only τ_2 will be measured. Similarly if $\tau_2 \ll \tau_1$, only τ_1 will be measured. Therefore, the simple unidirectional, un-

branched mechanism is inconsistent with the data unless the spectra of species A and B overlap.

Scheme III

$$A \underset{k_4}{\overset{k_3'}{\rightleftharpoons}} C \underset{k_2}{\overset{k_1'}{\rightleftharpoons}} B$$

Alternatively two intermediates can be generated from the ground state along two parallel paths as given in Scheme III, where both k_3' and k_1' are proportional to quantum yields and the light intensity. The rate equations are given by

$$-d[A]/dt \simeq k_1[A] - k_3\Phi_A[C_0] \sin \omega t \quad (A10)$$

and

$$-d[B]/dt \simeq k_2[B] - k_1\Phi_B[C_0] \sin \omega t \quad (A11)$$

The steady-state solutions are

$$[A] = \frac{(k_3/k_4)\Phi_A I_0[C_0] \sin (\omega t - \phi_1)}{(1 + \omega^2\tau_1^2)^{1/2}} \quad (A12)$$

and

$$[B] = \frac{(k_1/k_2)\Phi_B I_0[C_0] \sin (\omega t - \phi_2)}{(1 + \omega^2\tau_2^2)^{1/2}} \quad (A13)$$

where $\tau_1 = 1/k_4$, $\tau_2 = 1/k_2$, $\cos \phi_1 = k_4/(k_4^2 + \omega^2)^{1/2}$, and $\cos \phi_2 = k_2/(k_2^2 + \omega^2)^{1/2}$. This scheme readily accommodates the observation of two relaxation times with the appearance of only a single peak in the action spectrum. In terms of the usual bR nomenclature, C in Scheme III could be the bR ground state while A and B could be the fast- and slow-decaying forms of the M intermediate.

Registry No. CCCP, 555-60-2; La, 7439-91-0; NH_4Cl, 12125-02-9; H^+, 12408-02-5; nigericin, 28380-24-7; octyl β-D-glucopyranoside, 29836-26-8.

References

Becher, B. M., & Cassim, J. Y. (1975) *Prep. Biochem. 5*, 161–178.

Bell, D. H., Patterson, L. K., & Gould, J. M. (1983) *Biochim. Biophys. Acta 725*, 368–375.

Bernasconi, C. F. (1976) *Relaxation Kinetics*, Academic Press, New York.

Cerione, R. A., & Hammes, G. G. (1982) *Biochemistry 21*, 745–752.

Chang, C.-H., Chen, J.-G., Govindjee, R., & Ebrey, T. (1985) *Proc. Natl. Acad. Sci. U.S.A. 82*, 396–400.

Dewey, T. G. & Hammes, G. G. (1981) *Proc. Natl. Acad. Sci. U.S.A. 78*, 7422–7425.

Eigen, M., & De Maeyer, L. (1974) *Techniques of Chemistry* (Hammes, G. G., Ed.) Vol. VI, part II, pp 63–146, Wiley-Interscience, New York.

Goldschmidt, C. R., Ottolenghi, M., & Korenstein, R. (1976) *Biophys. J. 16*, 839–843.

Govindjee, R., Ebrey, T. G., & Crofts, A. R. (1980) *Biophys. J. 30*, 231–242.

Groma, G. I., Helgerson, S. L., Wolber, P. K., Beece, D., Dancsházy, Zs., Keszthelyi, L., & Stoeckenius, W. (1984) *Biophys. J. 45*, 985–992.

Hess, B., & Kushmitz, D. (1977) *FEBS Lett. 74*, 20–24.

Holloway, P. W. (1973) *Anal. Biochem. 53*, 304–308.

Huang, K.-S., Bayley, H., & Khorana, H. G. (1980) *Proc. Natl. Acad. Sci. U.S.A. 77*, 323–327.

Hwang, S.-B., & Stoeckenius, W. (1977) *J. Membr. Biol. 33*, 325–350.

Kano, K., & Fendler, J. H. (1978) *Biochim. Biophys. Acta 509*, 289–299.

Krupinski, J., Spudich, J. L., & Hammes, G. G. (1983) *J. Biol. Chem. 258*, 7964–7967.

Lanyi, J. K., & MacDonald, R. E. (1979) *Methods Enzymol. 56*, 398–407.

Lewis, A., Spoonhower, J., Bogomolni, R. A., Lozier, R., & Stoeckenius, W. (1974) *Proc. Natl. Acad. Sci. U.S.A. 71*, 4462–4466.

Li, Q.-Q., Govindjee, R., Ebrey, T. G. (1984) *Proc. Natl. Acad. Sci. U.S.A. 81*, 7079–7082.

Lin, J. T., Riedal, S., & Kinne, R. (1979) *Biochim. Biophys. Acta 557*, 179–187.

Lozier, R. H., Bogomolni, R. A., & Stoeckenius, W. (1975) *Biophys. J. 15*, 955–962.

Lozier, R. H., Niederberger, W., Bogomolni, R. A., Huang, S. B., & Stoeckenius, W. (1976) *Biochim. Biophys. Acta 440*, 545–556.

Oesterhelt, D., & Hess, B. (1973) *Eur. J. Biochem. 37*, 316–326.

Osterhelt, D. & Stoeckenius, W. (1974) *Methods Enzymol. 31A*, 667–678.

Ohno, K., Takeuchi, Y., & Yoshida, M. (1981) *Photochem. Photobiol. 33*, 573–578.

Sherman, W. V., Slifkin, M. A., & Caplan, S. R. (1976) *Biochim. Biophys. Acta 423*, 238–248.

Slifkin, M. A., & Walmsley, R. H. (1970) *J. Phys. E. 3*, 160–162.

Slifkin, M. A., & Caplan, S. R. (1975) *Nature (London) 253*, 56–58.

Stoeckenius, W., & Bogomolni, R. A. (1982) *Annu. Rev. Biochem. 52*, 587–616.

Stoeckenius, W, Lozier, R. H., & Bogomolni, R. A. (1981) in *Chemiosmotic Proton Circuits in Biological Membranes* (Skulachev, V. P., & Hinkle, P. C., Eds.) pp 283–309, Addison-Wesley, Reading, MA.

Ueno, M., Tanford, C., & Reynolds, J. A. (1984) *Biochemistry 23*, 3070–3076.

van Dijck, P. W. M., & van Dam, K. (1982) *Methods Enzymol. 88*, 17–25.

Westerhoff, H. V., & Dancsházy, Zs. (1984) *Trends Biochem. Sci. (Pers. Ed.) 9*, 112–117.